PERFORMANCE AND SAFETY OF ROOFTOP WIND TURBINES: USE OF CFD TO GAIN INSIGHT INTO INFLOW CONDITIONS

Amir Bashirzadeh Tabrizi[*a], Jonathan Whale[a], Thomas Lyons[b], Tania Urmee[a]

[a] *Physics and Energy Studies, School of Engineering and Information Technology, Murdoch University, Perth, WA 6150, Australia*

[b] *Atmospheric Science Studies, School of Veterinary and Life Sciences, Murdoch University, Perth, WA 6150, Australia*

Abstract

Installation of small and medium-size wind turbines on the rooftops of high buildings has been often suggested by architects and project developers as a valuable solution for achieving sustainable energy in building design. In such locations, however, because of the presence of buildings and other adjacent obstructions, wind is normally turbulent, unstable and weak, in terms of direction and speed. The use of wind turbines in the built environment pose challenges to overcome, including energy yield reduction due to lower mean wind speeds in urban areas and associated environmental impacts because of their close vicinity to the property and people.

There is a need to understand the inflow wind conditions for a small wind turbine in the built-environment. A resource assessment of the potential wind site in the built environment can determine the wind characteristics including zones of wind acceleration, recirculation, blocking and channeling. This knowledge is crucial for input into the design process of a small wind turbine to accurately predict blade fatigue loads and ensure that it operates safely with a performance that is optimized for the environment.

Computational Fluid Dynamics (CFD) is a useful method to model the wind flows in order to perform a resource assessment for the application of small wind turbines in a manner that requires less time and investment than a measurement campaign. This paper presents the results of research using a CFD code to model wind flow over the roof of a building and assess the possibility of combining a CFD package with a wind atlas software to form a wind energy resource assessment tool for the application of small wind turbines on the roof of a building. Experimentation with the model shows that the results are particularly sensitive to building height and shape, roof shape, wind direction, and turbine installation height and location. The results will be used to help develop a recommended practice of wind resource assessment in the built environment, in an international collaborative effort via the International Energy Agency Task 27.

Keywords: Small wind turbines, Built environment, CFD, Wind atlas software.

∗ Corresponding author. Tel.: +61893606713; e-mail: a.btabrizi@murdoch.edu.au.; address: School of Engineering and Information Technology, Murdoch University, 90 South Street, Murdoch, WA 6150, Australia

1. Introduction

A growing public awareness of the rising level of greenhouse gas emissions, the need to tackle fuel security and achieve reductions in emissions, has resulted in significant efforts to adopt renewable energy technologies in suburban environments [1,2,3]. The efforts have been increased in order to reduce the energetic demand of urban centres; specifically, small-size renewable energy systems represent an interesting solution for sustainable and reduced-energy in new building design [4].

Installation of small and medium-size wind turbines on the rooftop area of high buildings has been often suggested by architects and project developers as a valuable solution .Wind turbines integration into the built environment does pose challenges to be overcome the energy yield reduction resulted from lower mean wind speeds in urban areas and associated environmental impacts [5]. There have been some very public failures of small wind turbines in the built environment, notably in situations where the turbines have been mounted on top of the buildings [6,7,8]. Despite these problems, local governments and businesses continue to install SWTs on their rooftops as a dynamic, visible sign of support for renewable energy. It is thus vital to make the installations safe and to optimise performance to avoid them becoming bad advertisements for wind energy and renewable energy in general. To accomplish this, it is important to know the inflow wind conditions for SWTs in urban areas.

Due to the existence of obstacles with different shapes, high roughness length of the terrain and obstacles' interference to wind flow, wind conditions in urban locations are very complex and the adaptability of wind turbines to this environment is not yet tested both in terms of real power production and of structural compatibility with the buildings. As a result, the wind profile in urban locations is quite different from the classical log-law based profile [9].

At the sites of large wind turbines, performing comprehensive wind resource assessment yields knowledge about the characteristics of the lower part of the atmosphere as well as parameters like annual and seasonal average wind speed and turbulence characteristics. Turbulence is an important parameter to factor into wind turbine design as it causes cyclic loading on the blades and can lead to blade fatigue. In comparison, small-scale wind turbines are often located in more complex environments where the turbulence levels are higher and wind speeds are lower [10]. One of the most important differences between small-scale and large-scale wind turbines is that small-scale wind turbines are generally located where the power is required, often within a built environment, rather than where the wind is most favourable[4]. In understanding the inflow to a small wind turbine in the built-environment a resource assessment of the potential wind site can be used to determine the wind characteristics, including turbulence levels that the small wind turbine will have to experience. Recent research by the International Energy Agency (IEA) Wind RD&D Task 27, a vehicle for SWT research, has indicated that the turbulence design thresholds in the current international standard for SWTs, IEC61400-2 (ed. 3) are too low for SWTs in urban wind sites, and a better characterisation of turbulence is required for these kind of highly turbulent sites [11]

Wind resource assessments for large-scale wind projects typically involve lengthy and costly measurement campaigns. For small wind turbines application especially roof-top application, because of the small-scale of the projects, conventional site assessment methods are not always useful. First of all, compared to utility-scale or community-scale wind projects, small-scale roof-top urban projects do not typically have access to large amounts of fiscal resources

for the resource assessment phase of a project and thus investment in measurement equipment usually is limited. In addition, for urban environments, the traditional methods for wind energy site assessment are technically limited; the complex geometry can result to the situations where the resource varies substantially within a small area, thus a meteorological mast installed at a single location may not be a sufficiently good indicator of the overall resource within a complex environment. Also, the remote sensing technologies such as LiDAR are typically designed to work at 40 m or above and many small-scale roof-top urban projects are designed for deployment at lower heights. Computational Fluid Dynamics (CFD) techniques can be a reliable alternative for less expensive and faster resource assessments of roof-top small wind turbine applications and additionally provide physical insight to the governing flow mechanisms. Already, for modelling wind flows over complex rural terrains, modern CFD tools have proved essential [12].

Ledo *et al.* present a numerical study of wind flow above the roof in three suburban landscapes specified by houses with three different roof shapes; pitched , pyramidal and flat . They used a CFD technique to simulate the wind flow in such environments and to find the optimum turbine mounting locations. Their results show that the wind flow characteristics are strongly dependent on the shape of the roofs, with turbines mounted on flat roofs likely to generate higher and more reliable power for the same turbine hub elevation than the other roof profiles [2]. Heath, Walshe and Watson used CFD to model the flow characteristics within an urban area over an array of pitched-roof houses. They studied mean wind speeds at potential turbine mounting points and identified optimum mounting points for different prevailing wind directions. Also they proposed a methodology for estimating the energy yield of a building-mounted turbine from simple information such as wind atlas wind speed and building density. The results of the research show that the energy yield is very low when the turbine is installed below rooftop height [13]. Kalmikov and his team at Massachusetts Institute of Technology used CFD simulations to assess the wind energy potential on the campus of the Massachusetts Institute of Technology in Cambridge, MA. They enhanced the evaluation via integration of local wind measurements and observations from some nearby reference sites into the CFD model to estimate the local long-term climatology. Comparisons of measurements and simulated results provided validation of the modelling for mean wind speed, wind power density and wind variability parameterized by a Weibull distribution. Their work resulted to a better understanding of the micro-climate of wind resource on the MIT campus and addressed the optimal siting of a small turbine on campus [12]. Also CFD have been used by several researchers to evaluate the performancing of H-Darrieus small wind turbines on roof [9,14,15].

The ANSYS CFX 14 CFD software package[16] is used in this research to model wind flows over a building and is validated using secondary data from the CEDVAL wind tunnel datasets from Hamburg University. The CFD model of Bunning Group Ltd's warehouse at Port Kennedy in Western Australia was developed using the wind atlas software WAsP [17] to predict the wind velocities at the domain inlet. The research is novel as the CFD simulations are carried out on a building (the Bunnings warehouse) where there is an existing measurement system in place, allowing direct comparison between measurements and the model output. The research is also timely as it forms part of the current IEA Task 27 program of work that is looking at developing a Recommended Practice for micro-siting SWTs in the built environment [18]. The long-term research plan is to use this Recommended Practice is order to update the design classifications in the current IEC61400-2 standard to include a class for SWTs intended for use in highly turbulent sites such as in the built environment.

2. Aim and Objectives

The aim of this study is to gain an insight into the wind conditions for a SWT in the highly turbulent setting of the rooftop of a large building in order to provide guidance in the micro-siting of wind turbines. The specific objectives to achieve this aim are:

(1) Assess the combination of the CFD package CFX with the wind atlas software WAsP as a wind energy resource assessment tool for the application of small rooftop wind turbines in built environment.

(2) To use the combination of CFX and WAsP to investigate the local micrometeorological features of the wind flow and the effects of the complex urban topography via identifying zones of wind acceleration, recirculation and blocking. An understanding of zones of wind recirculation and turbulent wakes is important in terms of high energy production and protection of the machine from excessive loading from gusts by avoiding installation in such area.

In terms of the scope, this paper does not cover the investigation of wind power or turbulence kinetic energy on the rooftop.

3. Methodology

To assess the combination of a CFD package with the wind atlas software as a wind energy resource assessment tool in built environment area, a CFD model of Bunnings warehouse is created by means of CFX software, and the buildings around the warehouse up to 200 m radius were added to the model domain. The built-up area surrounding the warehouse is shown in Figure 1. To predict the wind velocity at inlet of CFD domain, the wind atlas software WAsP is used; raw data from the Kwinana Industries Council meteorological station located on Alcoa RDA Lake, taken between 12 August 2011 and 24 January 2012 are used as wind observations in WAsP. Figure 2 shows the location of the meteorological station compared to the location of Bunnings warehouse. WAsP was used to generate a regional wind atlas that included the mean wind speed of eight sectors N, NE, E, SE, S, SW and W at 200 metres above the ground. Because the wind characteristic for each sector at 200 metres above the ground is not affected by surface structures, it is used to predict the vertical wind profile. This profile was then used as the inlet velocity for the CFD model and the model was run for similar sectors to find the mean wind velocity on the roof of the warehouse. The results were extracted for the same dates as the ultrasonic measurements to allow for comparison. CFX assumes neutral atmospheric stability and thus the CFD results have been compared with neutrally stable wind data measured on the roof of Bunnings warehouse as well as with the whole measured data to check the accuracy of the combination of CFD and wind atlas software for rooftop wind resource assessment. To isolate the neutrally stable data, the wind measurements above the Bunnings rooftop are filtered by application of Golder's curve of Pasquill stability classes as functions of as Monin-Obukhov length, and roughness length [19]. The European wind atlas was consulted and the aerodynamic roughness of area around the Bunnings warehouse was estimated to be 50 cm.

Figure1- The built-up area surrounding the Bunnings warehouse in Port-Kennedy, Western Australia

Figure2- The location of Alcoa RDA Lake meteorological station compare to location of Bunnings warehouse in Port-Kennedy, Western Australia

3.1 Site and Measurement Campaign

The warehouse is a rectangular building, with its long-axis oriented NNE-SSW, a façade wall around the edge of the roof that is 8.4 m a.g.l, and a very low pitched roof (almost flat). The building is approximately 5 km from the coast (Indian Ocean) with the prevailing winds from the south-west. The warehouse is situated in a commercial estate but has no larger buildings or trees in the vicinity. Within a 1 km radius of the site there are mainly residential buildings to the north ,commercial and industrial buildings to the east and few buildings, low shrubs and low sand dunes to the south and west. The south-west front and the north-west side are comparatively open, though street furniture [1]and a car park exist on these sides [20].

A wind monitoring system was installed in September 2009 as part of a wind resource assessment for the installation of five small wind turbines that were later installed in March 2010. The Gill WindMaster Pro 3D ultrasonic anemometer was installed on a boom on a 5.3 m tall mast attached to the front-façade of the warehouse. The boom had a sliding collar in order to position the ultrasonic anemometer at different heights above the roof. The mast could be tilted down in order to make adjustments or to replace sensors. The data consists of 10Hz data over a six-month period (between 12/08/2011 and 24/01/2012). Figure 3 indicates the position of the ultrasonic anemometer on the roof.

Figure3- Position of the ultrasonic anemometer on the roof of Bunnings warehouse building in Port-Kennedy, Western Australia

1 Objects and pieces of equipment installed on streets and roads for various purposes

3.2 Computational Fluid Dynamic Model

3.2.1 Navier-Stokes equations and turbulence models

ANSYS CFX 14 developed by ANSYS, Inc., USA is used to perform the CFD simulations. Different methods such as Direct Numerical Simulation (DNS) [21]; Large Eddy Simulation (LES) [22,23], or the Reynolds-averaged Navier-Stokes (RANS) method with various turbulence models [24,25] have been applied in CFD simulations. The flow details that need to be obtained and the available computing resources are two critical criteria for choosing a proper method. Usually, it suffices to use the well-established RANS equations when only quasi-steady data is of interest, and that approach has been taken in the present study [2].

For modelling wind flow over complex terrain, the Reynolds-averaged Navier-Stokes approach (RANS) combined with a k-epsilon ($k-\varepsilon$) scheme as turbulence model, is the most common approach in wind engineering. The method provides a fair compromise between computational costs and accuracy. Reynolds decomposition is employed to the variables of the governing equations (each of them is divided in a time-averaged part and a fluctuating part,$u = \bar{u} + \acute{u}$) resulting to the two following equations:

$$\rho\left(\frac{\partial \bar{u}_i}{\partial t} + \bar{u}_j\,\frac{\partial \bar{u}_i}{\partial x_j}\right) = -\frac{\partial \bar{P}}{\partial x_i} + \rho \bar{g}_i + \frac{\partial}{\partial x_j}\left[\mu\left(\frac{\partial \bar{u}_i}{\partial x_j} + \frac{\partial \bar{u}_j}{\partial x_i}\right)\right] - \frac{\partial}{\partial x_j}\rho\overline{\acute{u}_i\acute{u}_j} \qquad (1)$$

$$\frac{\partial \bar{u}_k}{\partial x_k} = 0 \qquad (2)$$

The terms $\overline{\acute{u}_i\acute{u}_j}$ are known as the Reynolds stresses that physically represent the additional stresses because of the fluctuating components of the flow and modelled according to the 'Boussinesq' approximation, shown in Eq. (3). It is based on the analogy of Newton's friction law:

$$\tau_{ij} = -\rho\overline{\acute{u}_i\acute{u}_j} = \mu_t\left(\frac{\partial u_i}{\partial x_i} + \frac{\partial u_j}{\partial x_i}\right) + \frac{2}{3}\rho k\delta_{ij} \qquad (3)$$

where μ_t is called turbulent viscosity and $k = \frac{1}{2}\overline{\acute{u}_i\acute{u}_j}$ is the turbulent kinetic energy (TKE).

The 'standard' k-epsilon ($k-\varepsilon$) model, based on a two-equation turbulent energy scheme has represented a reasonable implement in approximately neutral atmospheric conditions. This model also provides an acceptable estimate of the turbulence intensity through the turbulent kinetic energy [26].

In this study, the CFX results converged much better using the Shear Stress Transport (SST) scheme. The SST scheme is a hybrid of two equation models that combines the advantages of both k-epsilon ($k-\varepsilon$) and k-omega ($k-\omega$) models. The SST k-ω equations are:

$$\frac{\partial \rho k}{\partial t} + \frac{\partial}{\partial x_j}\left(\rho U_j k\right) = \frac{\partial}{\partial x_j}\left[\left(\mu + \frac{\mu_t}{\sigma_{k3}}\right)\frac{\partial k}{\partial x_j}\right] + P_k - \beta'\rho k\omega + P_{kb} \qquad (4)$$

$$\frac{\partial \rho\omega}{\partial t} + \frac{\partial \rho\omega}{\partial x_j}(\rho U_j k) = \frac{\partial}{\partial x_j}\left[\left(\mu + \frac{\mu_t}{\sigma_{\omega 3}}\right)\frac{\partial \omega}{\partial x_j}\right] + (1 - F_1)2\rho \frac{1}{\omega \sigma_{\omega 2}} \frac{\partial k}{\partial x_j}\frac{\partial \omega}{\partial x_j} - \alpha_3 \frac{\omega}{k} P_k - \beta_3 \rho \omega^2 + P_{wb} \quad (5)$$

Where F_1 is a Blending function, P_k is turbulence production due to viscous forces [kg/ms^3], P_{kb} and $P_{\varepsilon b}$ are buoyancy production terms [kg/ms^3], α is a wind direction [°], β is sheltering effect factor ,$\sigma_{\omega 2}$ and $\sigma_{\omega 3}$ are constants in the SST k-ω turbulence model and finally ω is turbulent energy dissipation rate [1/s].

The SST k-ω model incorporates transport effects in the formulation of the eddy-viscosity and thus pays more attention to the transport of turbulence kinetic energy and predicts the starting and the size of the separation of flow under adverse pressure gradients more accurately than the standard $(k - \varepsilon)$ model. This leads to improvement of prediction of the flow separation, which is important in the present study [2].

3.2.2 Inlet wind profile

The velocity profile at the inlet boundary of the simulation domain must be accurately modelled to provide valid results of wind simulation in the built environment. The roughness of the ground affects the profile of wind velocity and therefore is necessary to be part of velocity profile simulation. The following equation is used to model the wind profile at the inlet of CFD domain:

$$u = \frac{u_*}{k} \ln\left(\frac{y + z_0}{z_0}\right) \quad (6)$$

where z_0 is the ground roughness of the simulated area, u_* is the friction velocity and *k* is von Karman's constant and is equal to 0.4. Since all the buildings within a radius of 200 metres around the target building have already been simulated in the CFD model, the ground roughness is set to 2 cm for all wind sector simulations. For each simulated sector, the mean wind speed at 200 meter above the ground (the output of the WAsP simulations) is used to find the friction velocity for the CFD simulation. Table 1 shows the results of the WAsP simulations in terms of mean wind speed for each sector.

Table 1
WAsP output: sector-wise mean wind speeds at 200 m.

Wind Sector	Mean wind speed (m/s)
North	6.36
North East	5.33
East	8.01
South East	7.57
South	8.53
South West	8.36
West	6.19
North West	6.18

3.2.3 Computational mesh

An unstructured tetrahedral mesh was used with five layers of 0.025 m inflation layer total thickness on the ground, roofs and walls of all buildings in all wind sector modelling. A cross-section of the mesh for the North wind sector is shown in Figure 4. The final mesh statistics in the models of eight wind sectors are shown in Table 2. The domain of CFX models for all simulated wind sectors were set up as a rectangular domain surrounding the urban grid.

Table 2
Final mesh statistics for all simulated wind sectors.

Wind Sector	Number of Elements	Number of Nodes
North	2121517	664904
North East	2475462	806925
East	2219394	707034
South East	1885504	594546
South	2511951	799133
South West	2104457	649320
West	2274320	719881
North West	1885504	594564

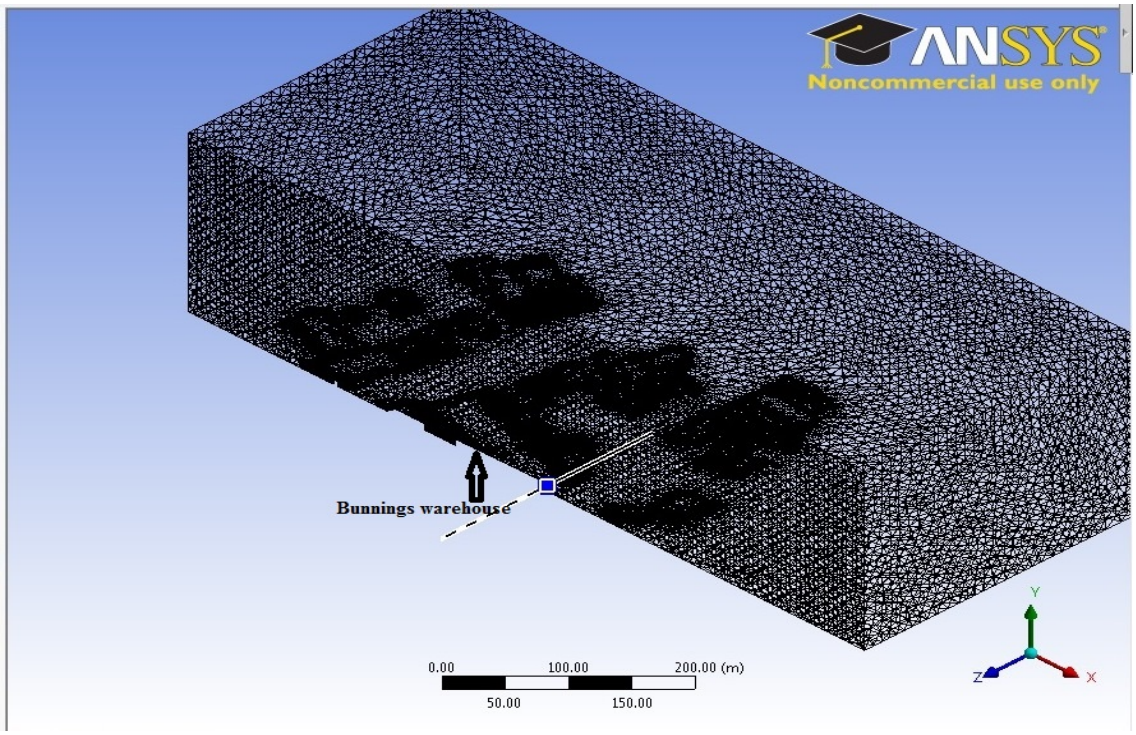

Figure 4-Cross-section of the mesh for North wind sector modelling of the Bunnings warehouse building in Port-Kennedy, Western Australia

3.2.4 Boundary domain and boundary conditions

For all wind sectors, the simulated buildings are placed in a rectangular domain of height equal to 200 meters and the lateral boundaries of the computational domain are at a distance of $5H_{max}$ away from the closest part of the built area at each side, where H_{max} is the height of the highest simulated building in the region of interest. A distance of $8H_{max}$ between the inflow boundary and the built area is applied as the longitudinal extension of the domain in front of the simulated region and 15 H_{max} behind the built area is employed to allow for flow re-development.

The turbulence level at the inlet boundary is adjusted to 5% (as suggested by CFX guidelines [16]). The downstream boundary was specified as an outlet with zero relative pressure and zero turbulence intensity gradients. Symmetric boundary conditions were employed for the side faces and top of the domain in all wind sectors. Solid boundaries including the ground of the domain and roofs and walls of the buildings have been set as no-slip walls with the CFX wall-function approach [27] used to model flow near these surfaces. An automatic near-wall treatment method is deployed by CFX to treat the wall effects. The near-wall treatment method accounts for the rapid variation of flow variables that occur within the boundary layer region as well as viscous effects at the wall. This treatment provides a smooth shift from low-Reynolds number formulation to wall function formulation.

4. Test Case: Flow around a Rectangular Obstacle

A test case was performed to model the flow around a rectangular structure to assess the accuracy of CFX in simulating flow around obstacles. The simulation results were then compared with the well-known CEDVAL wind tunnel datasets from Hamburg University. All data sets within the CEDVAL database follow a high quality standard in terms of complete documentation of boundary conditions and quality assurance during measurements [28]. The rectangular structure from the CEDVAL wind tunnel tests has dimensions of 125 mm height, 100 mm width and 150 mm length. The Reynolds number (*Re*) of the model test is 37,250 and the roughness length of the model is 0.007 m. The friction velocity and the offset height of model boundary layer is 0.377 m/s and 0 m respectively. The values of longitudinal and vertical wind components for 603 points in the vertical plane and the values of longitudinal and lateral wind components for 660 points in the horizontal plane have been provided in the data set. The data set also includes a visualization of flow around the structure in both horizontal and vertical planes.

The CFX simulation domain and obstacle was set up in a similar way to the configuration used in CEDVAL data set and the rectangular obstacle was meshed using a 125 mm cell edge length with two inflation layers of10 mm thickness near the walls. The wind flow through the model was set to give a *Re* of 37,250 as reported in CEDVAL data set and the same profile as equation (6) was used to simulate inlet velocity, setting z_0 equal to 0.007 m as the ground roughness of the model.

4.1 Test Case Validation

The comparison of numerical simulation results and corresponding experimental data with the aid of a metric is the core of CFX code validation. Therefore the hit rate, which is the

validation metric presented by the VDI guideline [29], is described here as it is used for test case validation.

A validation metric is a mathematical operator that specifies the accuracy of the results from numerical simulation by comparing them with results from experimental test [30]. The metric should supply information on the agreement, or disagreement, between the results of numerical simulation and experimental results. General and desirable features of metrics have been formulated by Oberkampf and Barone [31].

Experimental and simulation results should be available at the same positions to compute any metric, therefore the same points in the same plane as the CEDVAL data set have been generated in the simulation. Since the experimental measurement points don't typically coincide with the computational grid cell centres, interpolation of the numerical simulation results is essential. The validation metric hit rate, q, is calculated, after achieving the numerical results available at all experimental measurement positions [32,33].

In the permissible absolute difference, the uncertainty of measurement performs acts as a threshold while the relative difference becomes meaningless for experimental data approaching zero in the denominator (especially for lateral and vertical wind components that have very low normalised value) and therefore the permissible absolute error has been used in this study to calculate metric hit rate. The hit rate validation metric is the metric that is advised by the VDI guideline to be used for validating the numerical simulations and has been used in many previous investigations [34, 35, 36]. This is the main reason that the hit rate metric is used in the present work to test the CFX accuracy in simulating flow around obstacles.

According to VDI, 2005 [29], a hit rate of $q \geq 0.66$ for each velocity component is required to pass the validation test. This criterion is verified for the hit rates based on all valid measurement positions in the CEDVAL data set. Table 3 shows the hit rate values for longitude, lateral and vertical components of wind speed for simulated flow around the rectangular obstacle for the purposes of testing CFX accuracy.

Table 3
Hit rate values for wind components.

Item	Hit rate value (%)
Longitude wind component	73
Lateral wind component	82
Vertical wind component	79

As Table 3 presents, for all three wind components, the resulted hit rate value met the criteria and therefore the CFX model of flow around a rectangular obstacle is valid. This test case study shows that the CFX provides enough accuracy to simulate the flow around the obstacle and potentially a good tool for simulating the flow in built environment.

5. Results and Discussion

Table 4 shows the CFD simulated and measured results for the magnitude of the 10-minute averaged 3D velocity vectors on rooftop of Bunnings warehouse buildings for over the period 12 Aug 2011 and 24 January 2012, for various atmospheric conditions. The percentage of error between numerical results and measured results has been presented in the table for all wind sectors.

Table 4
CFD simulation and measured results on rooftop of Bunnings warehouse for 10-minute averaged wind speeds.

Wind Sector	CFD (m/s)	Measurement Neutrally Stable Condition(m/s)	Error (%)	No. of measured data- Neutrally Stable Data	Measurement Whole Data(m/s)	Error (%)	No. of measured data- Whole Data
N	4.3429	4.1347	5.0	76	3.3665	29.0	182
NE	2.4954	3.5827	-30.3	250	2.8780	-13.3	1068
E	3.7422	4.5182	-17.2	520	3.8198	-2.0	1861
SE	4.5900	4.2027	9.2	451	3.4711	32.2	1697
S	5.6381	4.5000	25.3	718	3.9313	43.4	1430
SW	5.8489	5.6998	2.6	955	5.3290	9.8	1752
W	4.6927	5.2132	-10.0	345	4.7421	-1.0	862
NW	4.3355	6.1329	-29.3	229	5.5433	-21.8	674

In terms of the neutrally stable atmospheric condition, the closest agreement between simulation and measurement (2.6%) is obtained for the south-west sector (prevailing wind direction). There is also reasonable agreement for north , south-east and west sectors, as well as the east sector as the error between simulation and measurement is less than 10%, and around 17%, respectively; The poorest agreement comes from the south, north-east and north-west sectors (errors around 25% or larger). The average error between simulation and measurement for all eight wind sectors is 16.1 precent. Table 4 shows a general trend that in most wind sectors that as the number of measured data points in a wind sector reduces (around or less than 1000) the error between simulated results and measured data increases. The large error in north-east sector despite the relatively not too low number of measured data in this sector, may be due to the of the fact that the five small wind turbines installed on the edge of Bunnings warehouse roof were simulated as five masts in CFX, and in reality have more effects on the wind in north-east sector. The discrepancy in results for north-west sector is likely to be due to a combination of lack of measured data from that sector together with the effect of some high light towers around the building that clearly cause some disturbance in the north-west sector not catered for in the CFD model. Finally, the small

distance between façade and measurement mast for cases when the wind comes from the south may be to the cause of the poor results for the south sector simulation as there is not enough distance between the façade and the mast in the CFD model to allow for flow re-development after the wind flow passes the façade before encountering the measurement mast.

In terms of comparison of the simulations with the whole set of measured data (across all atmospheric stability classes) the minimum error is 1.0 precent for the west wind sector and the numerical results for the north-east, south-west and east sectors are reasonable (the error is less than approximately 15 precent). For the north, south, north-west and south-east sectors, however, the simulation results are poor (errors around 21% or greater). The average error for all wind sectors is 19.1 precent.

As the values in Table 4 show, the combination of WAsP and CFX predicts neutrally stable flows over the building reasonably well, however the results are not good enough to predict the flow across the whole range of atmospheric conditions; Table 5 provides meteorological conditions defining Pasquill turbulence types [37]. Table 5 clearly shows that for most cases at wind speeds greater than 4 m/s the atmospheric condition is neutral. Since the wind speeds in the operating range of many small wind turbines would be above 4 m/s and thus dominated by neutrally stable atmospheric conditions, the findings of this paper suggest that the CFX/WAsP approach is a promising tool to predict wind speeds above the rooftops of buildings in the built environment. However, some caution needs to be used especially in the case of wind turbines with cut-in wind speeds lower than 4 m/s and in the case of strong-moderate daytime insolation levels.

Table 5
Meteorological conditions defining Pasquill turbulence types [37].

Surface Wind-Speed(m/s)	**Daytime Insolation**			**Nightime Conditions**	
	Strong	**Moderate**	**Slight**	**Thin overcast Or ≥ 4/8 low cloud**	**Cloudiness ≤ 3/8**
< 2	A	A-B	B	-	-
2-3	A-B	B	C	E	F
3-4	B	B-C	C	D	E
4-6	C	C-D	D	D	D
>6	C	D	D	D	D

Notes: A, extremely unstable; B, moderately unstable; C, slightly unstable; D, neutral (applicable to heavy overcast day or night); E, slightly stable; F, moderately stable; (for A-B take average of values for A and B, etc.)

Figures 5, 6 and 7 show some examples of output from CFX for the case of winds from the south-west sector, which is the prevailing wind direction. Figures 5a and 5b show the magnitude of wind speed contours on the long west-facing edge where the turbines and ultrasonic anemometer are installed and on the middle of the roof in the longitudinal sense of the Bunnings warehouse building, respectively. Contours of the wind velocity vertical component for the long west-facing edge and on the middle of the roof in the longitudinal sense of the building have been presented in Figures 6a and 6b respectively and Figures 7a, 7b show the wind velocity vectors on the long west-facing edge and on the middle of the roof in the longitudinal sense of the building. Comparison of Figure 5a and Figure 5b show that the magnitude of the wind velocity is slightly greater on the edge than in the middle of the roof. More marked is the difference in vertical wind components at the edge of the building

and the middle; the vertical components are much greater in the edge of the roof (Figures 6a and 7a) and this is clearly visible in from the contours for vertical wind components (Figures 6a and 6b) as well as the wind velocity vectors (Figures 7a and 7b). . These figures have an important consequence for small horizontal axes wind turbines (HAWTs) that are not designed to harness the vertical component of flow and in fact the vertical component of the wind velocity can have a significant effect on a HAWT in terms of fatigue loads. Therefore, the ideal location for installation of a machine, particularly a HAWT, should be in the middle of the roof of the Bunnings warehouse where the small wind turbine probably will experience lower loads due to vertical flow and will have a greater life time. Balduzzi *et al.* found that roofs with an inclination angle of 8 degrees were optimal in inducing a speed-up of flow over the building [9]. The sloping angle on the roof of the Bunnings warehouse is less than 8 degrees but, as Figure 8 suggests, the small inclination angle of the roof is effective to speed-up flow over the building and this is another reason for installation of small wind turbines in the middle of the roof for Bunnings warehouse building.

Figures 5b and 7b show that on the middle of the roof, the wind is slightly channelled after passing the short south-facing edge of the building and there is a zone of wind acceleration on top of the façade at this edge as well as a blockage zone behind the façade on the south-facing edge. There is a large recirculation zone behind the short north-facing edge of the building (Figure 7b) and this edge would be the worst place to install a wind turbine.

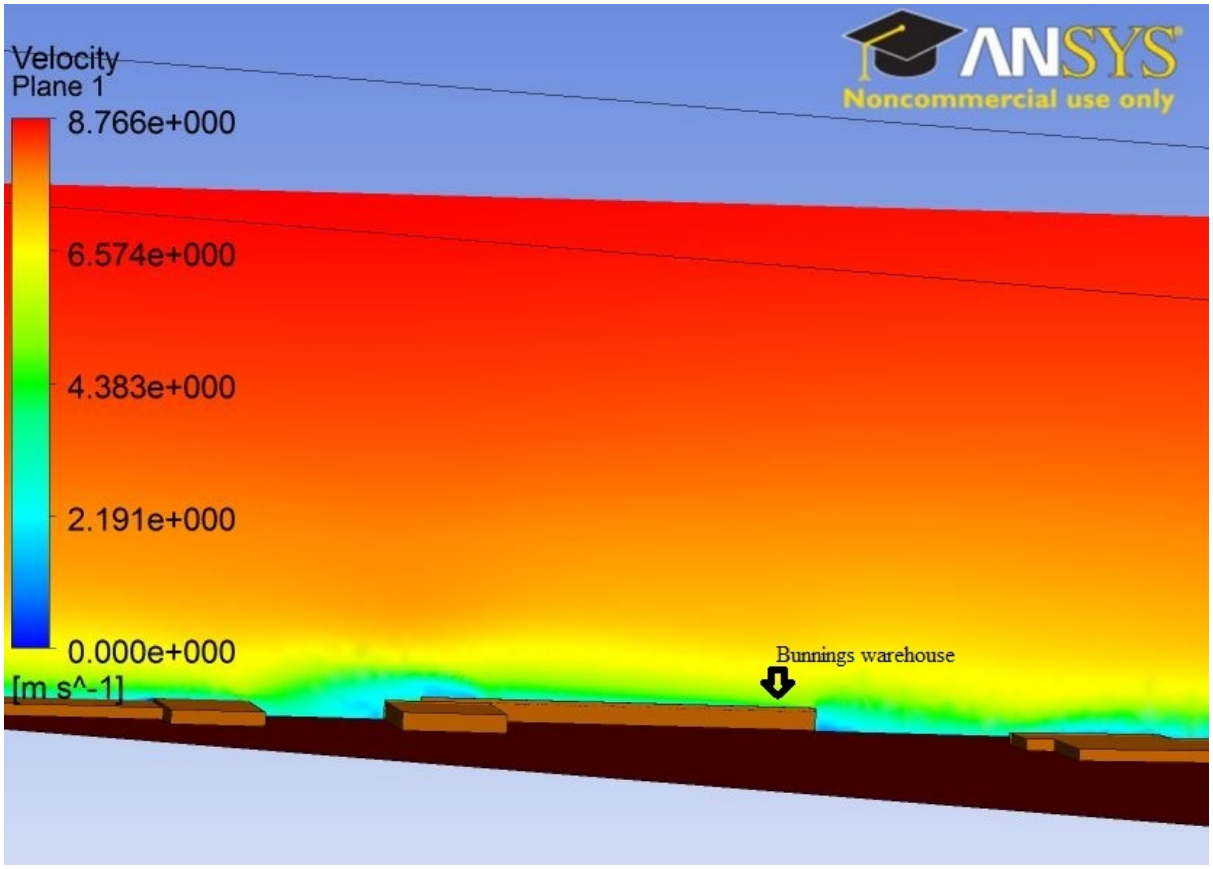

Figure 5a. Wind speed contours on the edge of the roof of the Bunnings warehouse building for the south-west wind sector simulation

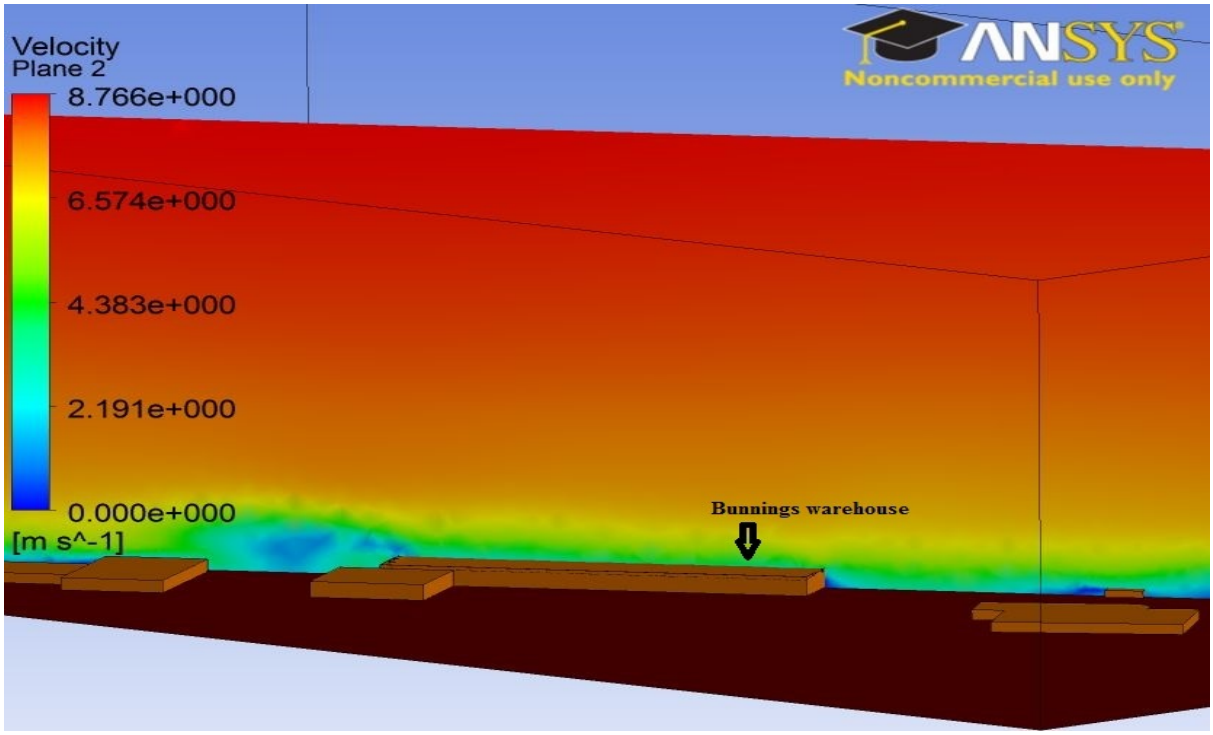

Figure 5b. Wind speed contours on the middle of the roof of the Bunnings warehouse building for the south-west wind sector simulation

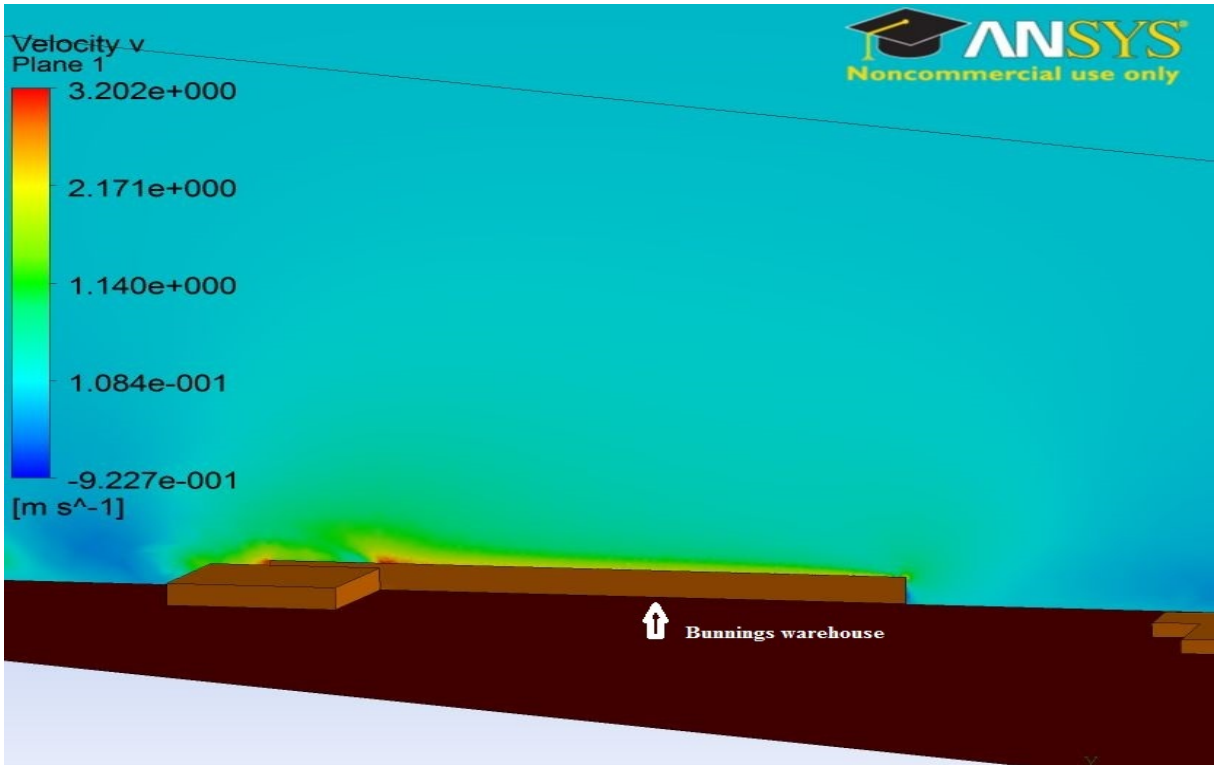

Figure 6a. Contours of vertical wind component on the edge of the roof of the Bunnings warehouse for the south-west wind sector simulation(Note that the vertical component is represented by v in CFX)

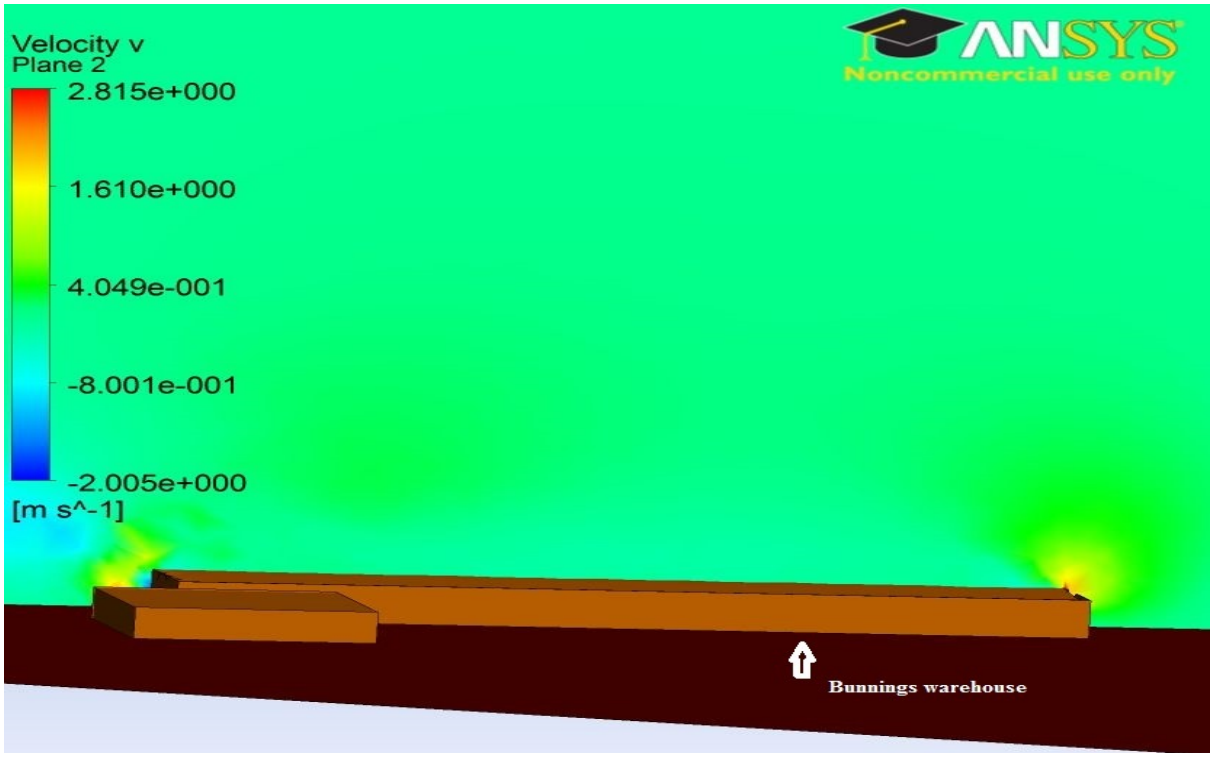

Figure 6b. Contours of vertical wind component on the edge of the roof of the Bunnings warehouse for the south-west wind sector simulation (Note that the vertical component is represented by v in CFX)

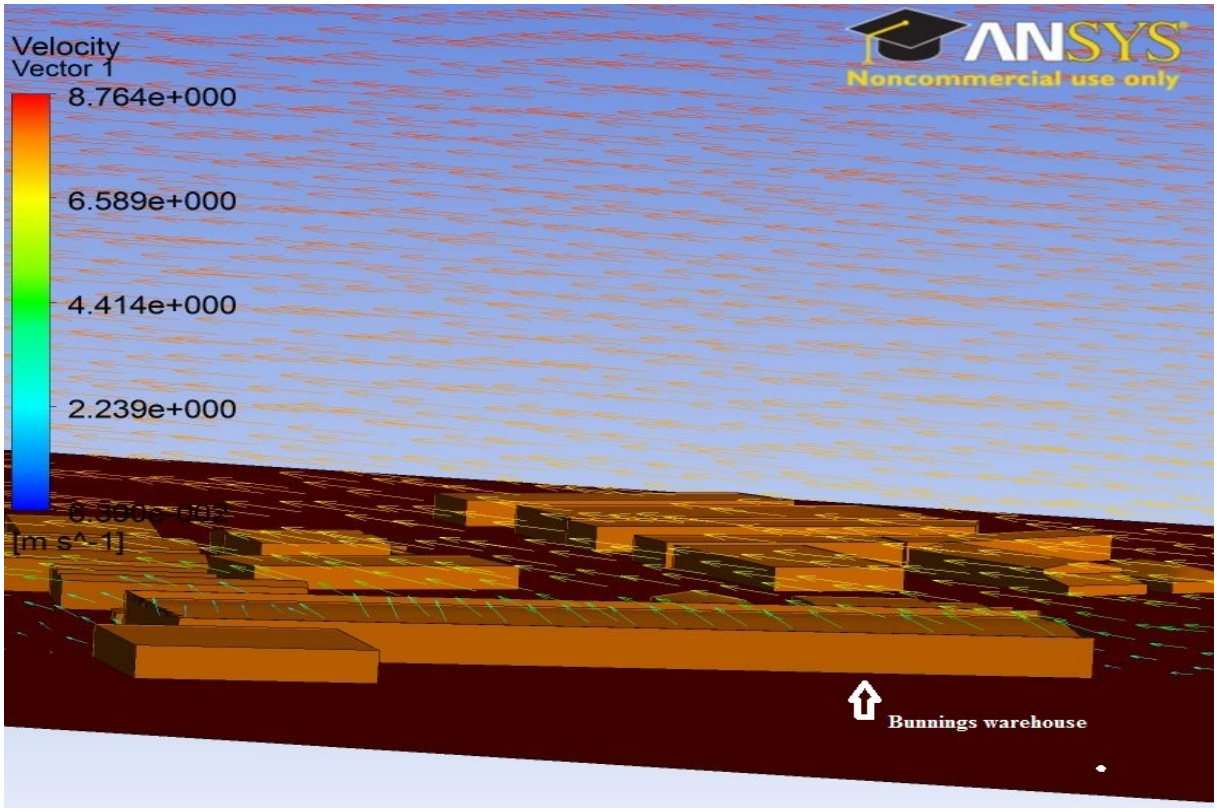

Figure 7a. Wind velocity vectors on the edge of the roof of the Bunnings warehouse for the south-west wind sector simulation

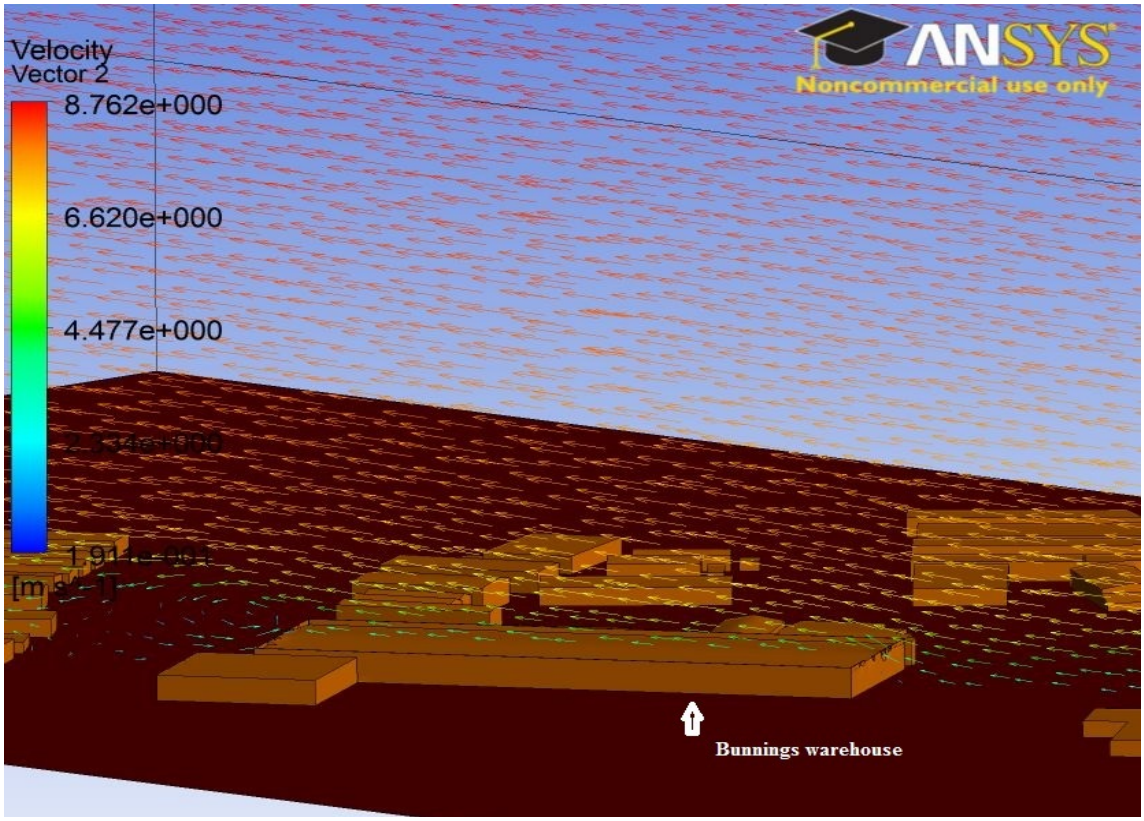

Figure 7b- Wind velocity vectors on the middle of the roof of the Bunnings warehouse building for south-east wind sector simulation (prevailing wind direction)

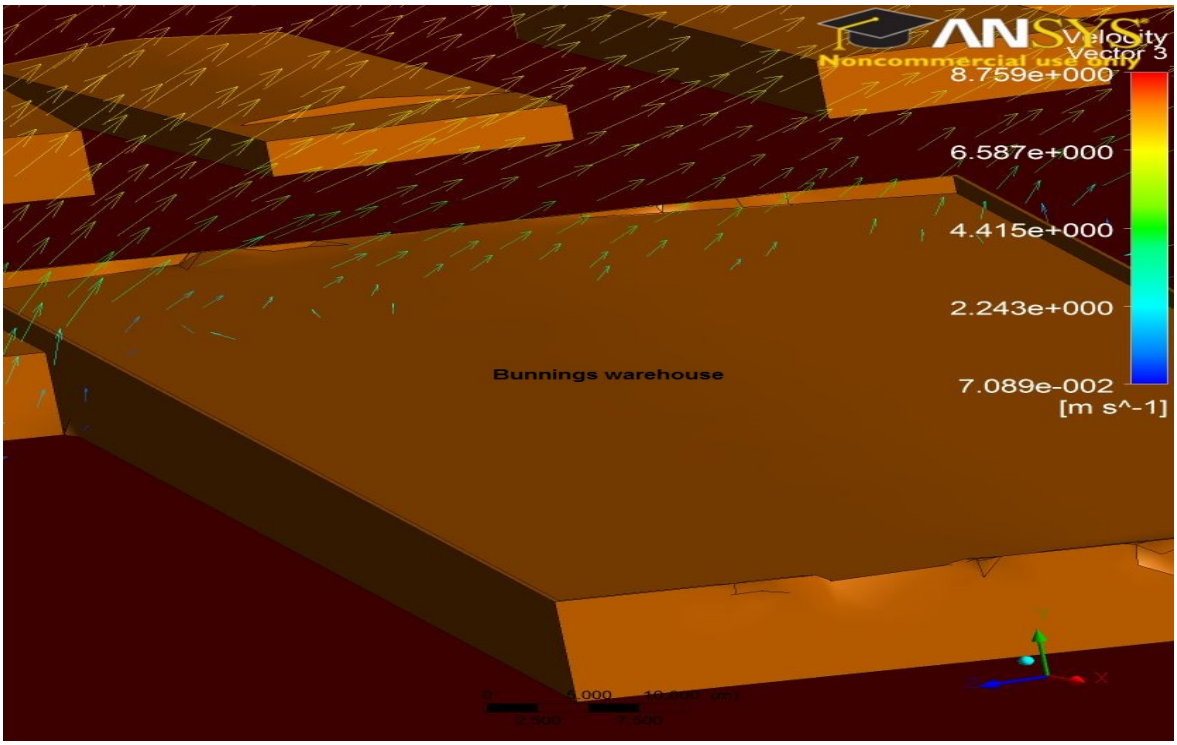

Figure 8- Effect of the sloping angle of the rooftop of the Bunnings warehouse in to speed-up flow over the building

Before drawing conclusions from this research, the limitations of the study must be noted. Firstly, only a few months of measured data have been taken (August to January) covering only the spring and summer seasons in the southern hemisphere. Definitely, a year long period of measured data on the rooftop would be preferable in order to consider seasonal effects. In addition, for the WAsP simulation the reference data have been taken from meteorological station 18 km away from the target building. This would be a source of error if the reference and target site do not have the same underlying regional wind climate.

6. Conclusion

In this study, the combination of a CFD package and wind atlas software was assessed as a wind resource assessment tool for a small wind turbine application on a rooftop in the built environment. The tool was used to investigate wind speed and direction on the rooftop of a building and identify the optimal location for installing small turbine taking into account zones of wind acceleration, recirculation and blocking. A CFD model of the Bunnings warehouse at Port Kennedy in Western Australia was created by means of the ANSYS CFX 14 package and the buildings around the warehouse up to a radius of 200 m was developed in the model geometry. The wind atlas software, WAsP was used to predict the wind velocity at the inlet of CFD domain. Observations for WAsP were taken from a metrological mast located 18 km from the Bunnings warehouse. The wind atlas resulting from the WAsP simulation was analysed to find the mean wind speed of eight sectors at 200 m a.g.l. and the mean wind speed for each sector was used to create a wind profile that was used as inlet flow to the CFD model. A wind monitoring system installed on the roof of the Bunnings warehouse at Port Kennedy was used to collect data for the CFD model validation. For model validation, the wind measurements above the Bunnings rooftop were filtered to select only neutrally stable wind data. To check the accuracy of the combination of CFD and wind atlas software for rooftop wind resource assessment, the 10-minute averaged mean velocity vectors from the simulations were compared with measured data.

The results of the study shows CFX provides reasonable accuracy for simulating flow around an obstacle and the combination of a CFD package with a wind atlas software such as WAsP provides a promising tool for wind resource assessments for small wind turbines on the roof of buildings. CFX predicts neutrally stable flows over the building well but further research are needed to understand how CFX results can be adjusted to predict flows across the whole range of atmospheric conditions. Having said that, most of the time when power is being generated by small wind turbines on the roof there are neutral atmospheric conditions and so the combination of a CFX with WAsP provides an applicable tool for wind resource assessment in terms of small wind turbines on rooftops.

The scope of this study was limited to wind speed and direction results. Further studies of turbulence intensity prediction on the roof are planned. In this case, modelling using a combination of an inflow turbulence simulator such as TurbSim and CFD packages such as CFX might be used. Accurate prediction of the turbulence intensity on the rooftop is very important for the application of small wind turbines in the built environment, because turbulence intensity is linked to fatigue on the machine and is mentioned as a basic parameter to characterise turbulence in IEC61400-2 standard on the design requirements for small wind turbines.

References:

[1] N. Carpman, Turbulence intensity in complex environments and its influence on small wind turbines, MSc Dissertation, Department of Earth Sciences, Uppsala University, 2011.

[2] L. Ledo, P.B. Kosasih, P. Cooper, Roof mounting site analysis for micro-wind turbines, Renewable Energy 36 (2011) 1379-1391.

[3] D. Ayhan, Ş. Sağlam, A technical review of building-mounted wind power systems and a sample simulation model, Renewable and Sustainable Energy Reviews 16 (2012) 1040-1049.

[4] F. Balduzzi, A. Bianchini, L. Ferrari, Microeolic turbines in the built environment: influence of the installation site on the potential energy yield, Renewable Energy 45 (2012) 163-174.

[5] S. Stankovic, N. Campbell, A. Harries, Urban Wind Energy, Earthscan, 2009.

[6] http://en.wikipedia.org/wiki/Wind_turbine.

[7] http://www.bergey.com/technical/warwick-trials-of-building-mounted-wind-turbines.

[8] http://www.cyclopicenergy.com/news / 20100812-TurbineFailureHobart/ Hobart-Marine-Board-Turbines.shtml.

[9] F. Balduzzi, A. Bianchini, E. A. Carnevale, L. Ferrari, S. Magnani, Feasibility analysis of a Darrieus vertical-axis wind turbine installation in the rooftop of a building, Applied Energy 97 (2012) 921-929.

[10] A. Makkawi, A.N. Celik, T. Muneer, Evaluation of micro-wind turbine aerodynamics: wind speed sampling interval and its spatial variation, Building Serv. Eng. Res. Technol. 30 (2009) 7-14.

[11] IEC 61400-2, Wind turbines-Part2: design requirements for small wind turbines-Annex M, Third edition, International Electrotechnical Commission, Geneva, Switzerland, 2011.

[12] A. Kalmikov, G. Dupont, K. Dykes, C. Chan, Wind power resource assessment in complex urban environments: MIT campus case-study using CFD analysis, AWEA 2010 WINDPOWER Conference. Dallas, USA, 2010.

[13] M.A. Heath, J.D. Walshe, Estimating the potential yield of small building-mounted wind turbines, Wind Energy 10 (2010) 271-287.

[14] S. Mertens, G.V. Kuik, G.V. Bussel, Performance of an H-Darrieus in the skewed flow on a roof. Solar Energy Engineering 125 (2003) 433–40.

[15] S. Mertens, The energy yield of roof mounted wind turbines, Wind Engineering 6 (2003) 507–517.

[16] http://www.ansys.com/Products/Simulation+Technology/Fluid+Dynamics/Fluid+ Dynamics+Products/ANSYS+CFX.

[17] http://www.wasp.dk.

[18] http://www.ieawind.org/task_27_home_page.html

[19] D. Golder, Relations among stability parameters in the surface layer, Bundary Layer Meteorol. 3 (1972) 47-58.

[20] M.S. Hossain, Investigating whether the turbulence model from existing small wind turbine standards is valid for rooftop sites, MSc Dissertation, School of Engineering and Energy, Murdoch University, Perth, 2012.

[21] S. Takahashi, J. Hamada, Y.K. Takashi, Numerical and experimental studies of airfoils suitable for vertical axis wind turbines and an application of wind-energy collecting structure for higher performance, Wind Engineering 108 (2006) 327-330.

[22] T. Uchida, Y. Ohya, Micro-siting technique for wind turbine generators by using large-eddy simulation, Wind Engineering and Industrial Aerodynamics 96 (2008) 2121-2138.

[23] M. Tutar, G. Oguz, Computational modelling of wind flow around a group of buildings, Computational Fluid Dynamics 18 (2004) 651-670.

[24] F.R. Menter, Two-equation eddy-viscosity turbulence models for engineering applications, AIAA Journal 32 (1994) 1598-1605.

[25] N.N. Sørensen, General purpose flow solver applied to flow over hills, PhD thesis, Risø-DTU, Lyngby,1995.

[26] J.A. Michelsen, Basis3D - a platform for development of multi-block PDE solvers, Technical Report AFM 92-05, Technical University of Denmark, Lyngby, 1992.

[27] ANSYS CFX-Solver theory guide release 14.5. ANSYS, Inc.; 2012.

[28] http://www.mi.uni-hamburg.de/Introducti.433.0.html.

[29] VDI, Environmental Meteorology-Prognostic Micro scale Wind field Models-Evaluation for Flow around Buildings and Obstacles, VDI Guideline 3783- Part9, Beuth Verlag, Berlin, 2005.

[30] W.L. Oberkampf, C.J. Roy, Verification and Validation in Scientific Computing, Cambridge University Press, New York, 2010.

[31] W.L. Oberkampf, M.F. Barone, Measures of agreement between computation and experiment: validation metrics, Computational Physics 217(2006) 5–36.

[32] VDI, Environmental Meteorology-Physical Modelling of Flow and Dispersion Processes in the Atmospheric Boundary Layer-Application of Wind Tunnels, VDI Guideline 3783- Part 12, Beuth Verlag, Berlin, 2000.

[33] J. Franke, M. Strum, C. Kalmbach, Validation of Open FOAM 1.6.x with the German VDI guideline for obstacle resolving micro-scale models, Wind Engineering and Industrial Aerodynamics 104-106 (2012) 350-359.

[34] K.H. Schluunzen, D. Hinneburg, O. Knoth, M. Lambrecht, B. Leitl, S. Lopez, C. Luupkes, H. Panskus, E. Renner, M. Schatzmann, T. Schoenemeyer, S. Trepte, R. Wolke, Flow and transport in the obstacle layer-first results of the micro-scale model MITRAS, Atmospheric Chemistry 44 (2003) 113–130.

[35] J. Franke, Application of Richardson extrapolation to the prediction of the flow field around building models, Proceedings of the 4th International Symposium on Computational Wind Engineering (CWE2006), Yokohama, Japan, 2006.

[36] J. Eichhorn, A. Kniffka, The numerical flow model MISKAM: state of development and evaluation of the basic version, Meteorologische Zeitschrift 19 (2010) 81–90.

[37] T.J. Lyons, W. D. Scott, Principals of air pollution meteorology, Belhaven Press,London,1990.